

Damage Estimation and Stress Singularity Study Using a Coherent Gradient Sensing Method

Joseph Scura¹, Rick Woods², Mark Sandor^{1,*}

¹Department of Mechanical Engineering, University of Newcastle, New South Wales, Australia

²Department of Mechanical Engineering Sciences, University of Surrey, Surrey, United Kingdom

Email address:

Mark.Sandor.Newcastle@gmail.com (M. Sandor)

*Corresponding author

To cite this article:

Joseph Scura, Rick Woods, Mark Sandor. Damage Estimation and Stress Singularity Study Using a Coherent Gradient Sensing Method.

Engineering Physics. Vol. 1, No. 1, 2017, pp. 8-13. doi: 10.11648/j.ep.20170101.12

Received: November 17, 2016; **Accepted:** December 13, 2016; **Published:** January 7, 2017

Abstract: In this paper, the stress singularity in homogenous material was studied using an optical experimental method. The study on stress concentration is of great research value to evaluate the damage inside materials. Coherent gradient sensing (CGS) is introduced to study the mechanical behavior of homogeneous material which was widely used in industry and research. The governing equations of CGS which is used to represent the optics-mechanics relation of the singular yield near the point of the external force are derived. The experimental result shows this CGS method as a nondestructive methodology is capable of estimating the load with high accuracy.

Keywords: Stress Singularity, Coherent Gradient Sensing, Damage Estimation, Optical-Mechanics

1. Introduction

Damage estimation is a challenging issue and requires an in-depth understanding of the material characteristics and response in multiscale under varying load and environmental conditions [1-5]. A lot of work has been done in this field to enhance the fidelity of damage assessment methodologies, using a wide range of sensors and detection techniques, for different kinds of materials [6-12]. However, detecting damage at the microscale is still challenging with commercially available sensors. One way to approach this issue is through accurate and efficient modeling techniques, which are capable of tracking damage initiation at the microscale and propagation across the length scales. A novel multiscale model has been developed by Zhang et al. to estimate the damage precursor of a smart polymeric material. [13, 14] In Zhang's work, a statistical network model is introduced, which is capable of bridging the high-accuracy molecular dynamics model at the nanoscale and the computationally efficient finite element model at the macroscale. The simulation and experimental results show that the multiscale network model is capable of capturing both local heterogeneous property and damage evolution. Another novel non-destructive technique, impact-echo method, was

developed by Ye et al. to detect damage in concrete structures. They performed experimental validation on real data collection to validated the propose approach. The comparison results demonstrated effectiveness of the propose method. [15, 16] Experimentally, traditional test methods using gauges and sensors are limited to detect stress in some locations for complex geometry and boundary conditions. Also, the size of gauge is another limitation to obtain accurate strain and stress information at the microscale. Therefore, a lot of work has been done to develop the structural health monitoring (SHM) which is critical to multidisciplinary application. [17-20] As a comprehensive technology, SHM integrates sensors and sensing techniques, damage detection algorithms, and prognosis for accurate estimation of component life. Compared with traditional experimental methods, the optical experimental methods are not only a nondestructive measurement but also capable of capturing whole stress/strain field information. Therefore, the optical mechanical experiment methods as a nondestructive testing method can be widely used to detect stress distribution and monitor local damage precursor.

Coherent gradient sensing (CGS) method has been widely used to study the stress singularity and estimate the damage evolution. In 1991, Tippur studied the governing function of

stress field using CGS method for the first time. [21] Bruck and Rosakis et al. discussed the accuracy, error and application of CGS in mechanical experiments and measurements. [22, 23] Lee et al. developed a comprehensive model of CGS technology and applied it to wider investigation based on Fourier optics. [24] Zhang and Yao used CGS method to study local singularity and fracture characterization of FGM and derived governing equations related to CGS measurement and elastic solution at mode I crack tip in terms of stress, material constants, and fringe order. [25] In CGS method, an optical circuit was designed using two parallel optical gratings which are set in a distance (see figure 1). This

circuit will generate the interference fringes which can be observed by a CCD. The sample will deform based on the external load and will result in different light path in this optical circuit. Therefore the interference fringe observed using the CCD can provide the strain field information of the sample surface using optical governing functions. The obtained interference fringe shape at crack tip consists of a series of dark and light rings (as shown in Figure 2). The size and shape of the dark/light rings can be used to detect the local strain field information at the microscale. The CGS method has a lot of advantages including nondestructive, setting up easily, insensitive to surrounding vibration and high accuracy.

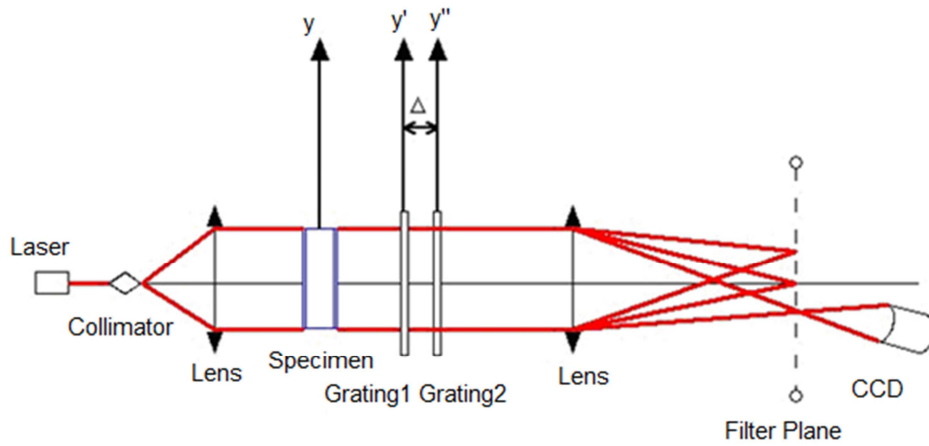


Figure 1. Optical circuit of coherent gradient sensing method.

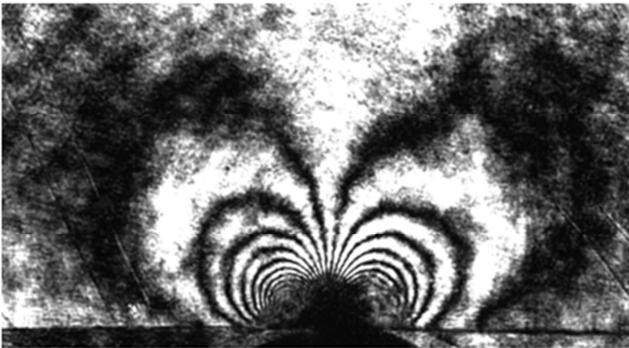


Figure 2. Interference fringe at crack tip using coherent gradient sensing method.

In this paper, the governing function of CGS method for a transmission circuit will be derived in section 2. The steps of the optical experiment will be introduced in section 3. The CGS experimental results will be discussed and compared with theoretical estimation in section 4.

2. Optical Experimental Methods

A transparent optical circuit was designed in this study. In this work, the x-axis is horizontal direction and y-axis is vertical direction in sample plane, z-axis is out-of-plane direction of sample. Figure 1 shows the optical circuit in this work which is from top view (y-axis). The external load

direction is gravity direction. For both gratings in this test, the principal direction of grating is parallel to x-axis, which is perpendicular to gravity direction. That means the grating line direction is parallel to y-axis, which is gravity direction. There is a relation between grating distance, pitch and orders of interference fringes (see Figure 3). The order and shape of the interference fringes can be used to indicate the material gradient and strain in this CGS method. The basic governing function of this optical experimental method can be described as [21]:

$$\frac{\partial w}{\partial y} = \frac{np}{2\Delta} \quad (1)$$

where w is the out-of-plane deflection of sample surface, n is order of interference fringes, p is grating pitch between neighbor lines, Δ is distance between the two gratings. The shift distance of diffraction light (on grating 2) diffracted by grating 1 can be described as:

$$\eta = \Delta \tan \varphi \approx \Delta \varphi \quad (2)$$

where, φ is diffraction angle and η is shift distance of diffraction light on grating 2 (see Figure 3). The diffraction angle, which is also related to grating property, can be described as:

$$\varphi = \sin^{-1} \frac{\lambda}{p} \approx \frac{\lambda}{p} \quad (3)$$

where, λ is wavelength of the laser and p is grating pitch. In the light circuits shown in Figure 1 and Figure 3, the optical path length difference of two neighbor beams diffracted after the two gratings can be described as:

$$\delta S(x, y + \eta) - \delta S(x, y) = n\lambda \quad (4)$$

where, $\delta S(x, y)$ and $\delta S(x, y + \eta)$ represent the optical path lengths of two neighbor beams, respectively; n is order of

interference fringes. Using Eqs. 2, 3 and 4, the relation between optical path length difference and order of interference fringes can be obtained:

$$\frac{\delta S(x, y + \eta) - \delta S(x, y)}{\eta} = \frac{n\lambda}{\eta} \quad (5)$$

Eq. 5 can also be described in differential format:

$$\frac{\partial [\delta S(x, y)]}{\partial y} = \frac{np}{\Delta} \quad (6)$$

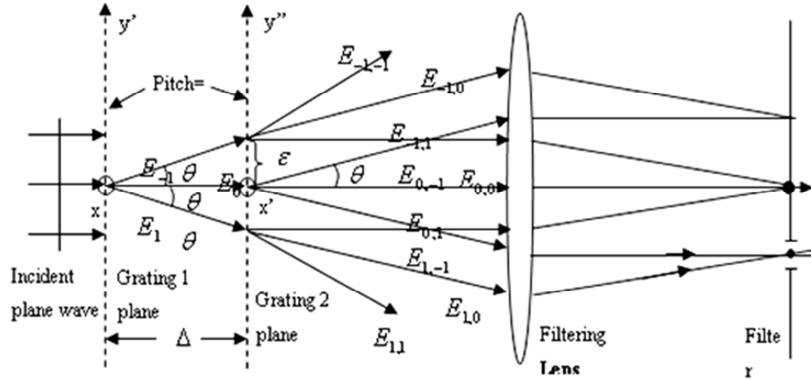


Figure 3. Schematic relation between grating distance, pitch and orders of interference fringes.

Here, the item $\frac{\partial[\delta S(x,y)]}{\partial y}$ can be used to describe the sensitivity of CGS method. Based on Eq. 6, the sensitivity of CGS method can be improved with a longer distance between two gratings and smaller grating pitch. In this test, the distance between gratings is 50 mm. For homogeneous material under linear load, the stress distribution can be described as:

$$\sigma_r = -\frac{2P}{\pi r} \cos \theta, \sigma_\theta = 0 \quad (7)$$

where, $\tilde{\sigma}_r$ and $\tilde{\sigma}_\theta$ are stress components in r and θ directions in polar system, P is linear load. Eq. 7 can be further described as:

$$\tilde{\sigma}_{11} + \tilde{\sigma}_{22} = \tilde{\sigma}_r + \tilde{\sigma}_\theta = -\frac{2P}{\pi r} \cos \theta \quad (8)$$

From Eq. 6 and Eq. 8, the relation between interference fringes and external linear load P :

$$P = \frac{n \cdot \lambda \cdot \pi \cdot \cos(2\theta)}{2 \cdot c \cdot \Delta \cdot r^2} \quad (9)$$

where, the interference fringes information can be described by polar system coordinates r and θ , and interference fringe order is n . Here the interference fringe order, n , can be either integer or integer plus 1/2. It represents light interference fringes when n is equal to integer (0, 1, 2 ...). And it represents dark interference fringes when n is equal to integer plus 1/2 (0.5, 1.5, 2.5 ...).

The CGS interference shape can be estimated using Eq. 9. The CGS interference in which the principal direction of both gratings were parallel to x -direction was shown in Figure 4. The CGS interference in which the principal direction of both gratings were parallel to y -direction was shown in Figure 5. In this model, the external load is applied on top of the sample is equal to 100N. The theoretical results show that the interference fringes of CGS are symmetric to y -axis. It consists of a series of ringlike curves for each part.

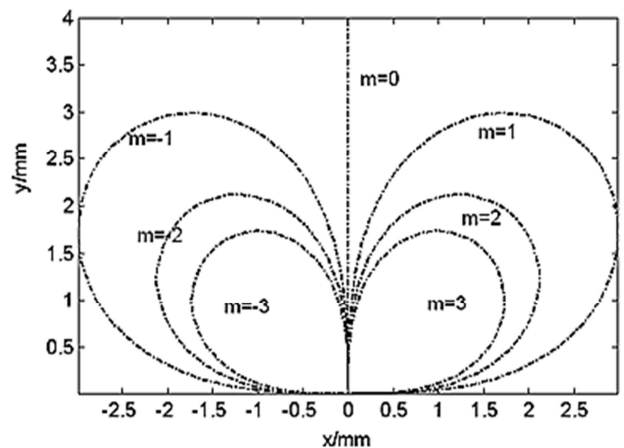


Figure 4. CGS interference shape with principal directions of both gratings parallel to x -direction.

In Figure 4 and 5, only the first four order of interference fringes were plotted ($n = 0, 1, 2,$ and 3). The higher order of interference fringe is in inner part. The diameter of ring-like

fringe will increase with a higher external load.

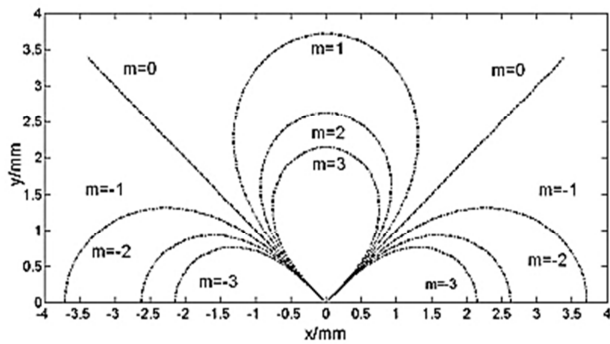


Figure 5. CGS interference shape with principal directions of both gratings parallel to y-direction.

3. Experimental and Simulation Results and Discussion

A transparent polyacrylamide sample is used in this study. The polyacrylamide material is considered as isotropic and homogenous. The material properties are listed in Table 1. The dimension of the sample is 100mm×40mm×6mm. A pre-crack, of which the length is 10mm, was set at the middle of the top surface, as shown in Figure 6. An external load is applied at

the position of the pre-crack, perpendicular to the sample top surface.

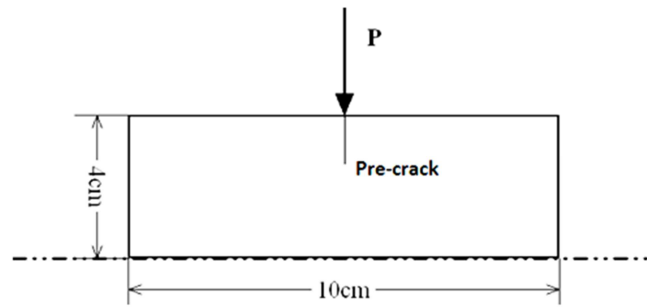


Figure 6. Sample geometry and external load.

Table 1. Material properties of the polyacrylamide.

Young's Modulus	Poisson's Ratio	Optical Parameter c
3.24 GPa	0.35	-1.08×10^{-10}

A numerical model was built to calculate the CGS fringe size based on Eq. 9. The simulation results for different loads were collected and compared with the optical experiment results, as shown in Figure 7.

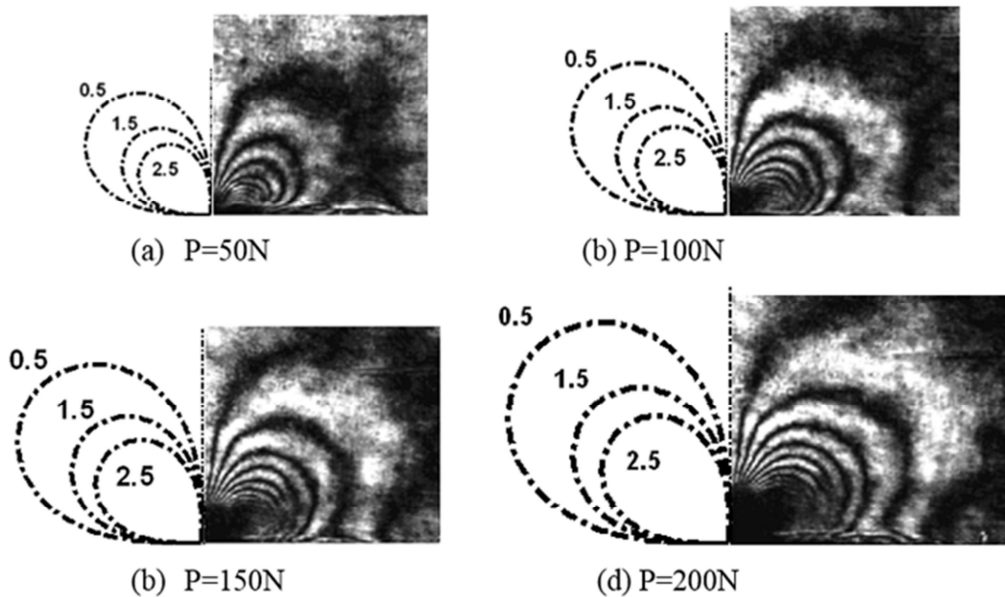


Figure 7. Comparison of experimental results and theory estimation using CGS method.

From Figure 7, the experimental CGS fringe size matches well with the simulation result calculated using Eq. 9. Therefore this optical methods is capable of evaluating the stress concentration at crack tip. The sizes of CGS fringes based on theory and test under different loads (from 0 to 200N) are compared in Figure 7. The error between test and theory are less than 5%. This result indicates the CGS method is very accurate to evaluate the local stress.

For the same order of CGS fringe, a series of points can be collected to estimate the external load using Eq. 9. However,

due to different r and θ values, the estimated load could be different for different positions in the CGS fringes. The relative error of load estimated using CGS method were plotted in Figure 8. It concludes that for order 1.5 the relative error could be minimized when θ is between 32° and 47° . For order 2.5 the relative error could be minimized when θ is between 45° and 55° . Overall, the relative error can be decreased under 5% when the points between 40° and 45° were collected.

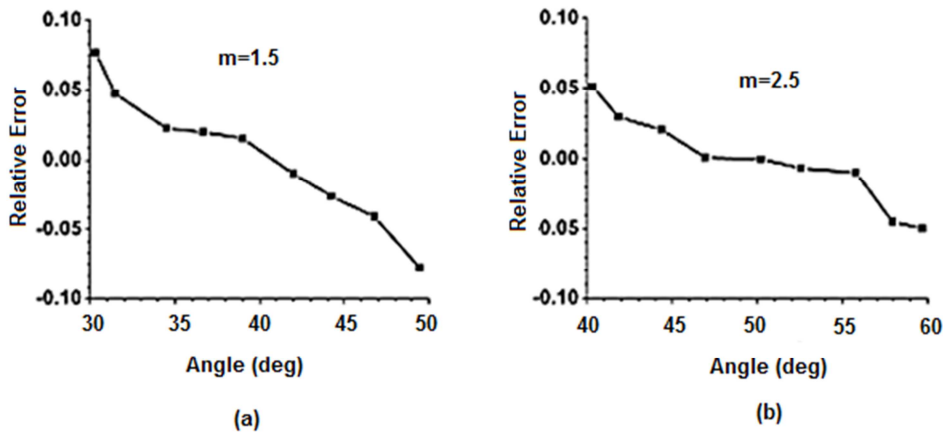


Figure 8. Relative errors of CGS method using different detective positions for a) CGS order is 1.5; b) CGS order is 2.5.

From Eq. 9, the external load can be calculated using the radius and angle of the CGS fringes obtained in the optical test. The comparison between estimated load using optical test and operating load is shown in Figure 9. The errors between estimated load using CGS method and operating load are less than 5% for order 0.5, 1.5 and 2.5. The results indicate the CGS method is capable to estimate the external force accurately.

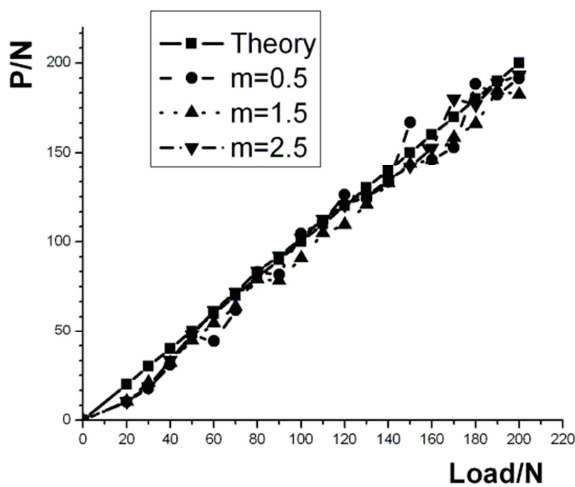


Figure 9. Comparison between estimated load (P) using CGS method and operating load.

There are a lot of advantages of the CGS method in the application of damage detection and load estimation. First of all, the CGS method is nondestructive. The test is all based on optical circuit. There is no sensors planted inside the sample or glued on the surface of the sample. So no damage or destruction are involved in the tested material. This provides the possibility to apply this novel optical methodology in the structural health monitoring to detect crack propagation in metallic and composite structures, which can be potentially implemented into airframe structures. Another advantage of the CGS method is this methodology is easy to set up. In the optical circuit, only one laser generator, two convex lens, and

one CCD are required. There is no strict requirement on the environment conditions like temperature, humidity and surrounding vibration. This provides the possibility to use this method in variable environment conditions. Also, as discussed before, the CGS method has very high accuracy. This is competitive to traditional test method using sensors. Finally, the governing function to estimate the external force or local stress is straightforward. The only input parameter to obtain the load is the diameter of the CGS. Therefore it is potential to be used in on-site monitoring and damage estimation.

The error in this CGS method can be attributed to several possible reasons. First, the external load applied on the sample surface is considered to be a line load in the governing function. But the contact surface between the indenter and sample surface in this test cannot be a line because of the limitation of the indenter size. This will result in some errors in the final results. Also, there is very high requirement of accurate optical circuit setting for CGS method. Therefore the accuracy of the dimensions in the optical circuit, such as the distance between two lens, lens and CCD, and lens and sample, will introduce some errors in the external load calculation. Besides that, the polyacrylamide material might be inhomogeneous and anisotropic locally at the crack tip at the microscale. The minor difference of actual material properties in crack tip and the material properties used in the governing function will introduce some errors. Finally, the accuracy of the measurement of the CGS size can result in some errors as well. The lower external load will result in smaller CGS size which is harder to measure accurately. This can also explain the reason the error will be reduced with a higher external load. Overall, the error between estimated load and operating load can be further reduced by using sharper indenter, setting accurate optical circuit, preparing high quality materials and improving the accuracy of the CGS measurement. The experimental results indicate the CGS method is capable to estimate the external force accurately.

4. Conclusion

In this paper, an optical experimental method of CGS

method was used to study the stress singularity issue. A numerical model was developed based on the optical governing functions to estimate the CGS fringes. The experimental results from CGS method were compared with theory and the CGS method was validated to be capable of estimating the external load. This study provides possibility to apply this optical method of CGS in nondestructive damage detection and structure health monitoring.

References

- [1] Atkinson C. and List R. D., "Steady state crack propagation into media with spatially varying elastic properties," *International Journal of Engineering Science*, 16, pp. 717-730, (1978).
- [2] Delale F. and Erdogan F., "The crack problem for a nonhomogeneous plane," *Journal of Applied Mechanics*, 50, pp. 609-614, (1983).
- [3] Zhang J., Gu J., Li L., Huan Y. and Wei B., "Bonding of alumina and metal using bulk metallic glass forming alloy," *International Journal of Modern Physics B*, 23, pp. 1306-1312, (2009).
- [4] Eischen J. W., "Fracture of nonhomogeneous materials," *International Journal of Fracture*, 34, pp. 3-22, (1987).
- [5] Huang G., Wang Y., and Yu S., "Fracture analysis of a functionally graded interfacial zone under plane deformation," *International journal of solids and structures*, 41, pp. 731-743, (2004).
- [6] Chalivendra V. B., Shukla A. and Parameswaran V., "Quasi-static stress fields for a crack inclined to the property gradation in functionally graded materials," *Acta Mechanica*, 162, pp. 167-184, (2003).
- [7] Jiansheng, G., Bingchen, W., Lei, L., Jinjun, Z., and Zhiwei, S., "Effect of Structural Relaxation on Hardness and Shear Band Features of Zr_{64.13}Cu_{15.75}Ni_{10.12}Al₁₀ Bulk Metallic Glass During Indentation", *Rare Metal Materials and Engineering*, S4, (2008).
- [8] Marur P. R., "Tippur H V. Evaluation of mechanical properties of functionally graded materials," *Journal of Testing and Evaluation*, 26, pp. 539-545, (1998).
- [9] Butcher R. J., Rousseau C. E. and Tippur H. V., "A functionally graded particulate composite: preparation measurements and failure analysis," *Acta Materials*, 47, pp. 259-268, (1999).
- [10] Parameswaran V. and Shukla A., "Processing and characterization of a model functionally gradient material," *Journal of Material Science*, 35, pp. 21-29, (2000).
- [11] Tippur H. V., Krishnaswamy S., Rosakis A. J., "A coherent gradient sensor for crack tip deformation measurements: analysis and experimental results," *International Journal of Fracture*, 48, pp. 193-204, (1991).
- [12] Bruck H. A. and Rosakis A. J., "On the sensitivity of CGS: Part I-A theoretical investigation of accuracy in fracture mechanics applications," *Optics and Lasers in Engineering*, 17, pp. 83-101, (1992).
- [13] Zhang J., Koo B., Liu Y., Zou J., Chattopadhyay A. and Dai L., "A novel statistical spring-bead based network model for self-sensing smart polymer materials," *Smart Materials and Structures*, 24, pp. 085022, (2015).
- [14] Zhang J., Koo B., Subramanian N., Liu Y. and Chattopadhyay A., "An optimized cross-linked network model to simulate the linear elastic material response of a smart polymer," *Journal of Intelligent Material Systems and Structures*, DOI: 1045389X15595292, (2015).
- [15] Ye J., Iwata M., Takumi K., Murakawa M., Tetsuya H., Kubota Y., Yui T., Mori K., "Statistical Impact-Echo Analysis Based on Grassmann Manifold Learning: Its Preliminary Results for Concrete Condition Assessment", *InEWSHM-7th European Workshop on Structural Health Monitoring*, 2014 Jul 8.
- [16] Ye, J., Iwata, M., Murakawa, M., Higuchi, T., Kubota, Y. and Yui, T., "Noise Reduction Methods for Hammering Impact Acoustic Inspection: An Experimental Comparison" *Structural Health Monitoring 2015*. (2015).
- [17] Parameswaran V. and Shukla V., "Crack-tip stress fields for dynamic fracture in functionally gradient materials," *Mechanics of Materials*, 31, pp. 579-596, (1999).
- [18] Giannakopoulos A. E. and Suresh S., "Indentation of Solids with gradients in elastic properties," *International Journal of Solids and Structures*, 34, pp. 2357-2392, (1997).
- [19] Zhang J., Liu K., Luo C. and Chattopadhyay A., "Crack initiation and fatigue life prediction on aluminum lug joints using statistical volume element-based multiscale modeling," *Journal of Intelligent Material Systems and Structures*, 24, pp. 2097-2109, (2013).
- [20] Zhang J., Johnston J. and Chattopadhyay A., "Physics-based multiscale damage criterion for fatigue crack prediction in aluminium alloy," *Fatigue & Fracture of Engineering Materials & Structures*, 37, pp. 119-131, (2014).
- [21] Tippur H. V., Krishnaswamy S., Rosakis A. J., "A coherent gradient sensor for crack tip deformation measurements: analysis and experimental results," *International Journal of Fracture*, 48, pp. 193-204, (1991).
- [22] Bruck H. A. and Rosakis A. J., "On the sensitivity of CGS: Part I-A theoretical investigation of accuracy in fracture mechanics applications," *Optics and Lasers in Engineering*, 17, pp. 83-101, (1992).
- [23] Bruck H. A. and Rosakis A. J., "On the sensitivity of CGS: Part II-An experimental investigation of accuracy in fracture mechanics applications," *Optics and Lasers in Engineering*, 18, pp. 25-51, (1993).
- [24] Lee Y. J., Lambros J., and Rosakis A., "Analysis of coherent gradient sensing (CGS) by Fourier optics," *Optics and Lasers in Engineering*, 25, pp. 25-53, (1996).
- [25] Zhang, J., Xu, W. and Yao, X.F., Load Detection of Functionally Graded Material Based on Coherent Gradient Sensing Method. *Journal of Mechanics*, pp.1-12, (2016).